Generalized van Vleck Perturbation Theory (GVVPT2) Study of the Excited States of Benzene and the Azabenzenes

Ajitha Devarajan,[†] Alexander V. Gaenko,[‡] Yuri G. Khait,[†,§] and Mark R. Hoffmann*[,†]

Chemistry Department, University of North Dakota, Grand Forks, North Dakota 58202, St. Petersburg State Institute of Technology (Technical University), 26 Moskovskii Ave, St. Petersburg 190013, Russia,and Russian Scientific Center "Applied Chemistry", 14 Dobrolyubova Ave, St. Petersburg 197198, Russia

Received: September 25, 2007; In Final Form: December 28, 2007

Generalized van Vleck perturbation theory (GVVPT2) for molecular electronic structures is applied to examine the azabenzene series: benzene, pyridine, pyrazine, symmetric triazine and symmetric tetrazine. The spectra of azabenzenes are complex with large numbers of excited states at low energies comprising n → π^* and π → π^* excited states and also doubly excited states of the n,n → π^*,π^* type. The calculations are complicated due to strong correlation effects in the nitrogen lone-pair orbitals and the π electrons. This study is the first to use GVVPT2 on conjugated systems. Comparison is made with experimental data and complete active space second-order perturbation theory, equation of motion coupled cluster and similarity transformed equation of motion coupled cluster theory data. Using polarized valence double split basis sets for benzene and pyrazine (cc-pVDZ) and pyridine (ANO-S) and polarized triple split basis sets (ANO-L) for triazine and tetrazine, the n → π^* and π → π^* states are computed with an average error of 0.28 eV in comparison with available experimental data.

1. Introduction

Generalized van Vleck perturbation theory[1] (GVVPT2) has been demonstrated to be a computationally efficient multireference perturbative method for the electronic structures of small molecules with results agreeing well with computationally more expensive methods[2−8] (e.g., MRCISD, CCSD(T)), but, to date, there have been no GVVPT2 investigations of conjugated systems. This study examines an important class of such molecules by studying the azabenzenes series: benzene, pyridine, pyrazine, symmetric triazine and symmetric tetrazine.

Benzene is the fundamental building block of aromatic systems and, as such, is of intrinsic interest. The azabenzenes are parent molecular systems for several compounds, such as the biologically active nicotinic acid and the nucleotides cytosine, uracil, and thymine, and have been the subject of extensive spectroscopic studies beginning with those of Innes et al.[9] More recently, UV and electron energy loss spectra have been reported by Palmer, Walker and co-workers and there have been some recent studies of Rydberg states.[10−12] In addition, a comprehensive collection of vacuum UV absorption spectra and theoretical data has also been reported by Bolovinos et al.[13] Where possible, the experimental excitation energies with which we compare are the peak intensity values (referred to as max energies), many of which are given by Bolovinos et al.,[13] who have also obtained several 0−0 (adiabatic) transition energies. A large number of 0−0 energies for azines have also been compiled by Innes et al.[9] The most successful prior multireference calculations on the azabenzenes are a series of complete active space perturbation theory (CASPT2) studies by Roos and co-workers.[14,15]

Initial examination of the azabenzene spectra shows similarities with the benzene spectrum; i.e., they show three bands located at approximately 5.0, 6.5 and 7.5 eV, respectively. Introduction of one or more nitrogen atoms in the benzene ring has two major effects on the UV spectrum: (1) splitting of the degeneracy of the E_{1u} state; (2) the introduction of new low-energy excited states associated with the n → π^* excitations. The presence of nitrogen lowers the symmetry of the molecules, so that transitions which are symmetry forbidden in benzene may become allowed in the azabenzenes. In general, it seems to be difficult to experimentally measure the energy separation corresponding to the splittings, and usually only one excitation is extracted from the measurements.

For pyrazine, six to eight excited states have been observed experimentally in the singlet and triplet manifolds. Assignments of these states have been suggested[13,15] and questioned.[16] It is interesting to note that the s-tetrazine molecule shows a host of dipole allowed transitions that have very diverse characteristics. The four nitrogen lone pair orbitals in s-tetrazine lead to a variety of low-lying n → π^* transitions and transitions to Rydberg states. Due to the rather low-lying π^* orbitals and the presence of a quartet of nitrogen lone pair orbitals, the s-tetrazine molecule has a number of low-lying excited states that either have significant n,n → π^*,π^* doubly excited character or are essentially pure doubly excited states. The theoretical description of the singlet part of the electronic spectrum of s-tetrazine is a challenge that requires a balanced treatment of the n,n → π^*,π^* double excitations.

To compute the excitation energies accurately, a balanced treatment of electron correlation is essential. Configuration state functions (CSFs) mixing the π electrons among the π orbitals describe the dominant correlation effects. In addition, the lone pairs of the nitrogen that may strongly interact with the π electrons also need to be considered on an equal footing. To obtain quantitatively correct results, dynamic correlation effects

* Corresponding author e-mail: mhoffmann@chem.und.edu.
[†] University of North Dakota.
[‡] St. Petersburg State Institute of Technology (Technical University).
[§] Russian Scientific Center "Applied Chemistry".

10.1021/jp077702w CCC: $40.75
Published on Web 02/14/2008

must be considered. However, as the complex near-degeneracy effects have been included already at the MCSCF level, treatment of the remaining correlation effects is normally faced with fewer complications and perturbation expansions can be expected to converge fast.

In the present study, we report results for the vertical excitation energies of the azabenzene series: benzene, pyridine, pyrazine, s-triazine and s-tetrazine using the GVVPT2 approach. Computational details are described in the next section. A discussion of the results for each molecule separately then follows, and a final section, which also includes discussion of features common to all molecules, concludes the paper.

2. Computational Methods

The GVVPT2 variant of multireference perturbation theory (MRPT) was used to describe the electronic structures of the ground and excited electronic states of the molecules in this study. GVVPT2 is a second-order, subspace-selective MRPT that can describe multiple states in a well-balanced manner. Since a complete description of the derivation and formalism of the GVVPT2 method has been given previously,[1] in this work we only review salient features. All calculations were performed using the GVVPT2 method as implemented in a local quantum chemistry program package (UND00).

In multireference based methods, the entire space in which a many electron wavefunction is expanded is partitioned into a "model space" containing the quasidegenerate reference function and perhaps other highly interacting functions and an "external space" connected with the model ones through electron excitations: $L = L_M \oplus L_Q$. Straightforward application of the most flexible multireference perturbation theory, the so-called "perturb-then-diagonalize" or effective Hamiltonian based methods, is faced with intruder state problems, where some of the external space states have energies that are close to those of high lying model space states. To circumvent the intruder-state problem, Kirtman[17] suggested that generalized van Vleck perturbation theories, in which "extended model spaces" are considered, be explored. These extended model spaces would include both the initial model space spanned by determinants that are expected to have large overlaps with the primary states of interest (i.e., the primary subspace, P) and some or all of the intruder states (i.e., the secondary subspace, S): $L_M = L_P \oplus L_S$. States in the secondary subspace, in contrast to the primary states, are not perturbatively corrected but are taken into account in the final diagonalization of the effective Hamiltonian in the total model space; hence, the secondary subspace forms a "buffer zone" between the states to be perturbatively corrected and the external space (Q). Figure 1 is a graphical depiction of the partitioning of the Hamiltonian.

In the GVVPT2 approach, a wave operator, $\Omega = UV$, is sought in which the $P-Q$ part of the wave operator, $U = \exp(X)$, which describes the interaction between primary states and the external states, is obtained perturbatively. Operator V describes interactions between the perturbed primary states and the unperturbed secondary states, and its matrix representation is obtained by solving the eigenvalue problem for the effective Hamiltonian,

$$\mathbf{H}^{\text{eff}}\mathbf{V} = \mathbf{V}\mathbf{E} \tag{1}$$

Operators U and V both depend on the primary space, and thus in principle must be searched for iteratively. Two of the authors[18] have shown that if a good initial approximation to the final primary subspace can be constructed (e.g., on the basis of state-averaged MCSCF calculations), no iterative process is required to obtain results of useful accuracy. In comparison with the intermediate Hamiltonian (IH) method of Malrieu and co-workers,[19] GVVPT2 and related methods do not require construction of the $Q-S$ block of the wave operator. In principle, the operators U and V are unitary; however, for low-order perturbation theories and for small perturbations, such as realized in practice with reasonable model spaces, the U operator is linearized, so that the actual effective Hamiltonian matrix that is used is given by

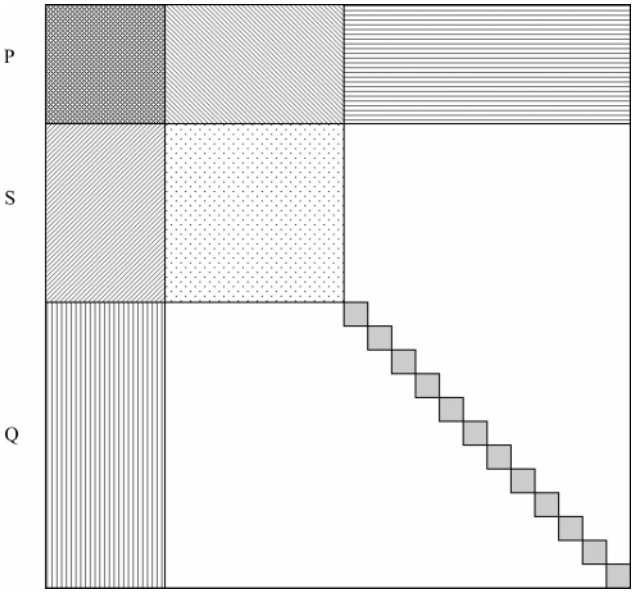

Figure 1. Graphical depiction of blocks of Hamiltonian relevant to the GVVPT2 method. See text for details.

$$\mathbf{H}^{\text{eff}}_{PP} = \mathbf{H}_{PP} + \frac{1}{2}(\mathbf{H}_{PQ}\mathbf{X}_{QP} + \mathbf{X}^{+}_{PQ}\mathbf{H}_{QP}) \tag{2}$$

$$\mathbf{H}^{\text{eff}}_{SP} = \mathbf{H}_{SQ}\mathbf{X}_{QP} \tag{3}$$

$$\mathbf{H}^{\text{eff}}_{SS} = \mathbf{H}_{SS} \tag{4}$$

In contrast to most other second-order MRPTs, including CASPT2, GVVPT2 does not assume that the $S-P$ block of the effective Hamiltonian is negligible. The coefficients of the first-order correction to the wavefunction, X_{qp}, can be viewed formally as arising from qp-pair dependent denominator shifts that rigorously eliminate singularities and are appropriate for both the nondegenerate and degenerate limiting cases, although conceptually as well as computationally it is better to consider the two effects separately:

$$X'_{qp} = -\frac{H_{qp}}{E^{(0)}_p - \tilde{E}^{(0p)}_q} \tag{5}$$

where $E^{(0)}_p$ is a Møller−Plesset-like zero-order energy of primary state p and $\tilde{E}^{(0p)}_q$ is a shifted zero-order energy of external space CSF q,

$$\tilde{E}^{(0p)}_q = \frac{1}{2}(E^{(0)}_q + E^{(0)}_p) - \frac{1}{2}\sqrt{(E^{(0)}_q - E^{(0)}_p)^2 + 4\sum_{q' \in m_e} H_{q'p}{}^2} \tag{6}$$

where $E^{(0)}_q$ is the Møller−Plesset-like zero-order energy of external CSF q and the summation is over all CSFs with the

same electron configuration ($\mathbf{m}_e$) as q. Then, the actual first-order correction to the wavefunction is related to this intermediate quantity by

$$X_{qp} = \tanh(\tilde{E}_q^{(0p)} - E_p^{(0)})X'_{qp} \quad (7)$$

It is useful to note that, although complicated, this formula results in energies that are continuous functions with respect to nuclear coordinates and do not involve any arbitrary, system dependent parameters.

The GVVPT2 method does not impose any restrictions on the CSFs that span the model space; hence, the model space can be complete or incomplete. A general procedure for dividing the set of molecular orbitals into groups and assigning allowed occupancies to the groups (i.e., the so-called "macroconfiguration approach"[20]) can produce significant computational efficiencies in the context of multireference perturbation theory, and the current second and third order[8,21] generalized van Vleck perturbation theory (GVVPT2 and GVVPT3) programs utilize this approach. The macroconfiguration based approach allows the efficient use of incomplete model spaces and thus extends the range of the molecular systems that can be investigated. For the present studies, the model spaces were complete; nonetheless, the use of multiple macroconfigurations to define a CASSCF space produces significant savings in the correlated treatment because of the efficient prescreening of Hamiltonian matrix elements.

Calculations were performed at geometries available in the literature from previous high level calculations or from experimental data. The geometry for benzene was taken from the NIST Computational Chemistry Comparison and Benchmark Database[22] ($R_{C-C} = 1.399$ Å, $R_{C-H} = 1.093$ Å). For pyridine and s-triazine, we have taken MP2(frozen core)/6-311G** optimized geometries from the NIST Computational Chemistry Comparison and Benchmark Database.[22] (pyridine, $R_{C1-N} = 1.343$ Å, $R_{C2-C3} = 1.398$ Å, $R_{C3-C4} = 1.396$ Å, $R_{C2-H} = 1.088$ Å, $R_{C3-H} = 1.086$ Å, $R_{C4-H} = 1.086$ Å, $\angle$NCC = 123.9°, $\angle$HCN = 115.8°, $\angle HC_3C_4 = 121.2°$; s-triazine, $R_{C-N} = 1.339$ Å, $R_{C-H} = 1.087$ Å). The geometry of the pyrazine molecule has been taken from the work of Weber and Reimers[23] ($R_{C-N} = 1.332$ Å, $R_{C-C} = 1.396$ Å, $R_{C-H} = 1.082$ Å, $\angle$NCC = 122.1°, $\angle$HXX = 120.7°). For the s-tetrazine molecule we have taken CASPT2-optimized geometry from the work of Schütz et al.[24] ($R_{C-N} = 1.338$ Å, $R_{N-N} = 1.324$ Å, $R_{C-H} = 1.073$ Å, $\angle$NCN = 126.5°).

For benzene, an active space consisting of six π orbitals was used, whereas for the azabenzenes the active space used consisted of six π-orbitals and nitrogen atom lone pairs. The number of electrons in the active space was thus $(6 + 2n)$, where n is the number of nitrogen atoms in the molecule. Consequently, the resulting model space can be expected to provide qualitatively correct descriptions of most, if not all, low-lying excited states. Separate state-averaged CASSCF calculations for each irreducible representation and multiplicity, with equal weighting of states, were used in all studies to generate the molecular orbitals and describe the nondynamic correlation; subsequent GVVPT2 calculations were performed for each symmetry and multiplicity with primary spaces comprised of the MCSCF functions. For benzene and pyrazine, for which previous calculations showed relatively close agreement with experiment, the cc-pVDZ basis set[25] was used; pyridine, for which we were concerned with some Rydberg transitions, was described with the ANO-S basis;[26] and triazine and tetrazine, which previous calculations showed as having larger discrepancies between theory and experiment, were described with the ANO-L basis.[27] All 6 Cartesian components of the d-functions were used in all calculations.

TABLE 1: Vertical Excitation Energies (in eV) for Benzene

sym	CASPT2[a]	GVVPT2	expt[b]
$^1B_{2u}$	5.02	5.02	4.90
$^3B_{1u}$	4.18	4.16	3.89
$^3E_{1u}$	4.86	4.83	4.85
$^3B_{2u}$	5.69	6.02	5.69

[a] Reference 28. [b] References 30 and 31.

3. Results and Discussions

3.1. Benzene. The UV spectrum of benzene is dominated by excitations to the B_{2u}, B_{1u} and E_{1u} states, all associated with $\pi \rightarrow \pi^*$ excitations. Excitations to the two lower energy states are symmetry forbidden, while the excitation to the E_{1u} state is symmetry allowed and a strong band is observed.

State averaging over two states in each symmetry and multiplicity was considered at the CASSCF level, and, in GVVPT2, the primary space is composed of these two low-lying states. Since our programs can only take advantage of Abelian point groups, calculations on the molecule used the D_{2h} subgroup of the full D_{6h} symmetry.

Comparison of the computed vertical excitation energies and band maxima should be made with care. Roos and co-workers have earlier studied the vibronic spectra of the lowest singlet states of benzene and found that the band maximum for the $^1B_{2u}$ state appeared at 0.12 eV higher energy than the most intense vibrational band, suggesting that 0.1 eV should be added to the experimental values.[28,29] The excitation energies for benzene calculated with the GVVPT2 method are compared with experimental data,[30,31] and CASPT2 results (using the same active space but a triple-ζ basis set) and are given in Table 1. It should be noted that the GVVPT2 values, although unshifted, are in good agreement with experimental values.

3.2. Pyridine. The computed and the experimental excitation energies and oscillator strengths for pyridine are reported in Table 2. Two optically allowed transitions have been observed in the energy range of 3.5−5.8 eV with band maxima located at 4.59[32] ($^1B_1$) and 4.99 eV[13] ($^1B_2$). These values differ by at most 0.15 eV from the values published by Walker et al.[11] The first state is of n $\rightarrow \pi^*$ type, while the second corresponds to the $^1B_{2u}$ state of benzene. The 0−0 transition energy for the $^1B_1$ state is 4.31 eV.[9,13] CASPT2 places the vertical excitation energies of the $^1B_1$ and $^1B_2$ states at 4.91 and 4.94 eV, respectively. We performed CASSCF and GVVPT2 calculations for four, two and three states for the A_1, A_2 and each of B_1 and B_2 symmetries, respectively. In general, more CASSCF functions are included in the primary space than the number that is of interest: the high-lying functions serve to stabilize the calculation and are not necessarily reasonable representations of the high-lying states; we report energies for states that are well-supported by the model space. The calculation of high-lying states, while possible in the GVVPT2 framework, would require a different model space. Our computed values for the $^1B_1$ and $^1B_2$ states, calculated using the ANO-S basis, are 4.98 and 4.85 eV, respectively (*cf.* Table 2). STEOM-CC calculation places the $^1B_2$ state at 4.82 eV.[33] Walker et al. recorded electron energy loss spectra and detected three optically forbidden transitions in the same energy region (4.1, 4.84, 5.43 eV), but they do not give an assignment.[11]

An earlier CASPT2 study by Fülscher et al.[15] with the ANO-L basis and a larger active space ($8\pi+4n$) suggested that the transition to the $^1A_2$ state might give rise to the scattering

TABLE 2: Vertical Excitation Energies (in eV) for Pyridine

state	sym	CASPT2[a]	STEOM-CC[b]	GVVPT2	expt max (0−0)
$\pi \rightarrow \pi^*$					
	$^1B_2$ ($^1B_{2u}$)	4.94	4.82	4.85	4.99[c]
	$^1A_1$ ($^1B_{1u}$)	6.35	6.62	5.79	6.38[c]
	$^1A_1$, $^1B_2$ ($^1E_1$)	6.84, 7.49	7.29	7.65, 7.14	7.22[c]
	$^1A_1$, $^1B_2$ ($^1E_2$)	7.78, 7.84		8.75, 9.13	8−9[c]
$n \rightarrow \pi^*$					
	$^1B_1$	4.91		4.98	4.59[d] (4.31[c,e])
	$^1A_2$	5.21		5.49	5.43[f]

[a] Reference 15. [b] Reference 33. [c] Reference 13. [d] Reference 32. [e] Reference 9. [f] Reference 11.

TABLE 3: Vertical Singlet Excitation Energies (in eV) for Pyrazine

state	sym	CASPT2(10,8)[a]	EOM-CCSD(T)[b]	SAC-CI SD−R[c]	GVVPT2	expt[d,e] max (0−0)
$n \rightarrow \pi^*$						
	$^1B_{3u}$	3.58	3.95	4.25	4.05	4.20 (3.83)
	$^1B_{2g}$	5.17	5.57	6.04	5.55	(5.46)
	$^1B_{1g}$	6.13	6.62		6.08	6.10
	^1A_u	4.37	4.81	5.24	4.35	
$\pi \rightarrow \pi^*$						
	$^1B_{2u}$	4.77	4.64	4.84	4.92	4.81 (4.69)

[a] Reference 15. [b] Reference 34. [c] Reference 35. [d] Reference 12. [e] Reference 13.

features at 5.43 eV. Our result for the $^1A_2$ state at 5.49 eV is in accordance with this assignment. The main peak of the second band corresponds to an A_1 state and appears in the UV spectrum at 6.38 eV.[13] Our calculated excitation energy for this state is 5.79 eV. The major peak in the strongest optical band, the third excited $\pi \rightarrow \pi^*$ state, is observed at 7.22 eV[13] and is a composite of excitations with $^1A_1$ and $^1B_2$ character. GVVPT2 excitation energies to $\pi \rightarrow \pi^*$ states of A_1 and B_2 symmetries in this region are 7.65 and 7.14 eV, respectively. STEOM-CC calculations predict the $^1E_{1u}$ excitation energy at 7.29 eV.[33] These results are also in agreement with the EOM-CCSD(T) results of Del Bene et al.[34] Broad absorption is seen in the range of 8−9 eV.[13] The calculated high energy $^1A_1$ and $^1B_2$ (E_{2g}) excitations, 8.75 and 9.13 eV, respectively, fall into this region. It is therefore likely that the corresponding bands are hidden under the Rydberg transitions.

3.3. Pyrazine. The introduction of a second nitrogen atom into the pyridine ring results in additional $n \rightarrow \pi^*$ states and lowering of the first $n \rightarrow \pi^*$ band in the experimental spectrum. The experimental 0−0 energy for this $^1B_{3u}$ state is reported as 3.83 eV.[13] We performed CASSCF and GVVPT2 calculations for two states of each symmetry. Results of the present GVVPT2 calculations for five singlet states are compared with other theoretical calculations and available experimental values (*cf.* Table 3). For the low-lying singlet valence $n \rightarrow \pi^*$ excited states, $^1B_{3u}$ $^1B_{2g}$ and $^1B_{1g}$, GVVPT2 calculated them at 4.05, 5.55, 6.08 eV, respectively. The GVVPT2 excitation energies are in good agreement with the experimental values (the errors are 0.15, 0.09, 0.02 eV, respectively).[9,13] Excitation energy values computed at EOM-CCSD(T)[34] and SAC-CI SD-R[35] levels agree well with the GVVPT2 results. We predict that one state of ^1A_u symmetry falls between the $^1B_{3u}$ and $^1B_{2g}$ states, with a computed energy of 4.35 eV. This agrees with the earlier CASPT2 prediction for this state at 4.37 eV.[15] EOM-CCSD(T) calculations places this state at 4.81 eV.[34] The lowest $\pi \rightarrow \pi^*$ excitation is observed at 4.81 eV, and our computed value is 4.92 eV for this state. CASPT2, obtained using a triple-ζ level basis set and different active spaces for $n \rightarrow \pi^*$ and $\pi \rightarrow \pi^*$ excitations, obtains 4.77 eV. EOM-CCSD(T) and SAC-CI SD-R calculated this energy to be at 4.64 and 4.84 eV, respectively.[34,35]

The six lowest triplet states of pyrazine have been determined by a variety of experimental and theoretical techniques, with the most recent work being that of Walker and Palmer.[12] Weber and Reimers have computed energies for all six states using *ab initio* and density functional methods.[23] The three lowest $n \rightarrow \pi^*$ states are observed at 3.42 ($^3B_{3u}$), 4.20 (^3A_u), and 4.59 eV ($^3B_{2g}$), respectively.[12] The three lowest $\pi \rightarrow \pi^*$ states were observed at 4.00 ($^3B_{1u}$), 4.5 ($^3B_{2u}$) and 5.7 eV ($^3B_{1u}$), respectively.[12] Our GVVPT2 results are presented in Table 4 along with earlier CASPT2, SAC-CI SD-R and experimental data.[13,23,35] For the three $n \rightarrow \pi^*$ states ($^3B_{3u}$, ^3A_u,$^3B_{2g}$), GVVPT2 results perform better on average than SAC-CI SD-R and CASPT2.[23,35] Errors with respect to the experimental data are 0.06, 0.09 and 0.28 eV, respectively. CASPT2 errors for these states are 0.18, 0.22 and 0.15 eV, respectively. For the three triplet $\pi \rightarrow \pi^*$ excited states ($^3B_{1u}$, $^3B_{2u}$ and $^3B_{1u}$), GVVPT2 overestimates the $^3B_{1u}$ state compared to CASPT2 and SAC-CI SD R.[23,35] For the $^3B_{2u}$ state, the GVVPT2 results coincide with CASPT2 and are better than those of SAC-CI SD-R. For the $^3B_{1u}$ state, GVVPT2 results are in better agreement with the experimental data than CASPT2 and SAC-CI SD-R.[13,23,35]

TABLE 4: Vertical Triplet Excitation Energies (in eV) for Pyrazine

state	sym	CASPT2(10,8)[a]	SAC-CI SD-R[b]	GVVPT2	expt[c,d] max (0−0)
$n \rightarrow \pi^*$					
	$^3B_{3u}$	3.24	3.82	3.36	3.42
	^3A_u	4.42	5.34	4.29	4.2
	$^3B_{2g}$	4.84	5.39	4.87	4.59
$\pi \rightarrow \pi^*$					
	$^3B_{1u}$	4.15	4.25	4.32	4.00
	$^3B_{2u}$	4.32	4.12	4.32	4.5 ± 0.1
	$^3B_{1u}$	5.04	5.14	5.36	5.7 ± 0.2

[a] Reference 23. [b] Reference 35. [c] Reference 12. [d] Reference 13.

3.4. s-Triazine. The present calculations have been carried out in C_{2v} symmetry instead of the full D_{3h} symmetry of the molecule. When selecting MOs for the $6\pi+3n$ active space for s-triazine, a diffuse $4b_1$, which is a Rydberg type orbital, was omitted and the $5b_1$ π-orbital was taken instead. CASSCF and GVVPT2 calculations for four states of each symmetry were performed.

Excitation energies computed using GVVPT2, and the ANO-L basis, are compared with experimental and earlier

TABLE 5: Vertical Excitation Energies (in eV) for s-Triazine

state	sym	CASPT2[a]	EOM-CCSD(T)[b]	GVVPT2	expt max[c]
$\pi \rightarrow \pi^*$					
	$^1A_2'$	5.33	5.36	5.70	5.70
	$^1A_1'$	6.77	6.90	7.28	6.86
	$^1E'$	8.16	7.72	7.40($^1A_1$) 7.35($^1B_2$)	7.76
$n \rightarrow \pi^*$					
	$^1A_1''$	3.81	4.49	4.21	
	$^1A_2''$	4.00	4.54	4.19	4.59
	$^1E''$	4.21	4.56	4.32($^1A_2$) 4.57($^1B_1$)	3.97

[a] Reference 15. [b] Reference 34. [c] Reference 13.

theoretical investigations in Table 5. Three $\pi \rightarrow \pi^*$ absorption lines were observed in the UV spectrum of s-triazine, with the first of them, the $^1A_2'$ peak, located at 5.7 eV.[13] We computed this line to be at 5.70 eV, which is in obviously fortuitously perfect agreement with the experimental observation. Earlier theoretical results using EOM-CCSD(T) and CASPT2 underestimate this state by 0.37 and 0.34 eV, respectively.[15,34] The second absorption maximum, arising due to a transition from the ground to the $^1A_1'$ state, is located at 6.86 eV; this transition is optically forbidden. We computed this energy difference to be 7.28 eV (i.e., 0.42 eV overestimate). The earlier CASPT2 study by Fülscher et al. used a larger 12π orbital active space and reported 6.77 eV for this peak. This suggests that this high-lying state requires a larger active space. EOM-CCSD and EOM-CCSD(T) calculations places this state at 7.30 and 6.90 eV respectively.[34] The first $^1E'$ state is observed at 7.76 eV, and GVVPT2 calculates this state at 7.38 eV (i.e., error of 0.39 eV). Similar errors of 0.40 and 0.31 eV were reported with the CASPT2 and EOM-CCSD calculations. EOM-CCSD(T) calculates this state to be at 7.72, in excellent agreement with the experiment.[34] The errors for all methods are still well within 0.5 eV, which is a useful accuracy for predictions involving high-lying states. Better agreement with EOM-CCSD and excellent agreement by EOM-CCSD(T) suggest that higher order dynamic correlation including triples is important for this state.

Experimentally, two $n \rightarrow \pi^*$ transitions have been observed and assigned: 3.97 ($^1E''$) and 4.59 eV ($^1A_2''$).[13] We have computed the excitation energies of $^1E''$ and $^1A_2''$ at 4.45 eV (arithmetic average of $^1A_2$ and $^1B_1$ is used) and 4.19 eV, respectively. A similar error of around 0.5 eV (actually, 0.6 eV) was reported for $^1A_2''$ state with the CASPT2 study. EOM-CCSD and EOM-CCSD(T) calculate this state at 4.95 and 4.54 eV, respectively.[34] Innes et al.[9] quote an estimate of 4.09 eV for the $^1A_2''$ state 0−0 transition. The presence of the first $^1A_1''$ in the same region is suggested by Innes et al. and is in agreement with our theoretical results. This unobserved state is placed at 4.49 eV by EOM-CCSD(T) calculations. CASPT2 calculates this state at 3.81 eV[15,34] while the present GVVPT2 calculated the excitation energy for this state is 4.21 eV.

3.5. s-Tetrazine. As with the s-triazine study, the present calculations used the ANO-L basis. When selecting MOs for the active space for s-tetrazine, the protocol of Schütz et al.[24] was used, in which the diffuse $2b_{2g}$ π-orbital was omitted and instead a $3b_{2g}$ π-orbital was taken. We performed CASSCF and GVVPT2 calculations for three states of A_g, B_{1g}, B_{3g}, B_{2u} and B_{3u} symmetries, for two states of B_{2g} and A_u symmetries and for four states of B_{1u} symmetry.

The visible region of the electronic spectrum of s-tetrazine, responsible for its reddish-purple color, is very unusual, with over 500 strong peaks reported, grouped in four intense vibrational progressions.[36,37] Computed GVVPT2 results for the singlet $n \rightarrow \pi^*$ and $n,n \rightarrow \pi^*,\pi^*$ excited states are compared with experimental and recent *ab initio* (CASPT2 and ext-STEOM-CC) results in Table 6.[38−42]

TABLE 6: Vertical Excitation Energies (in eV) for Low-Lying Singlet Valence $n \rightarrow \pi^*$ (S) and $n,n \rightarrow \pi^*,\pi^*$ (D) Excited States of s-Tetrazine

sym	CASPT2[a]	Ext-STEOM-CC[b]	GVVPT2	expt VUV (EEL)
1^1B_{3u} (S)	1.96	2.22	2.01	2.25[c] (2.35[d])
1^1A_u (S)	3.06	3.62	3.09	3.4[e] (3.6[d])
2^1A_g (D)	4.37	5.06	4.34	
1^1B_{1g} (S)	4.51	4.73	4.47	
1^1B_{2g} (S)	5.05	5.09	4.92	
1^1B_{3g} (D)	5.16	5.06	5.26	
2^1A_u (S)	5.28	5.23	5.32	(5.0[d])
2^1B_{2g} (S)	5.48	6.16	5.78	
2^1B_{1g} (S)	5.99	7.06	6.20	
2^1B_{2u} (S)	6.37	6.53	6.58	6.34[d] (6.4[d])
3^1B_{1g} (S)	6.20	6.70	6.60	

[a] Reference 40. [b] Reference 41. [c] Reference 9. [d] Reference 39. [e] Reference 42.

From emission spectroscopy, it was concluded that the visible absorption is related to the lowest singlet state.[38] The 1^1B_{3u} state is the lowest singlet excited state of s-tetrazine, and corresponds to an $n \rightarrow \pi^*$ transition. The maximum of the band is observed at 2.35 eV in the EEL spectrum.[39] Rubio and Roos[40] in their CASPT2 study suggest 1.96 eV for the vertical excitation energy of this state, and the present GVVPT2 study predicts this state to be located at 2.01 eV. The extended STEOM-CC study by Nooijen places this state at 2.2 eV.[41] The second singlet excited state is the optically forbidden 1^1A_u state. Innes has estimated this state to be located at 3.4 eV above the ground state.[42] While Nooijen's extended STEOM-CC reports this state at 3.62 eV, Rubio and Roos report this state to be located at 3.06 eV.[40,41] We have computed this state to be located at 3.09 eV above the ground state. Two optically forbidden states are predicted to lie more than 4 eV above the ground state, which could explain the origin of the second $n \rightarrow \pi^*$ band. The 2^1A_g state, described mainly by a doubly excited configuration, has been computed in the present GVVPT2 study to be at 4.34 eV. The forbidden 1^1B_{1g} state has been located at 4.47 eV. The calculated values are closer to the corresponding CASPT2 values of 4.37 and 4.51 eV, respectively, than to the extended STEOM-CC values.

The EEL spectrum observed by Palmer et al.[39] shows features at 4.2, 4.6 (shoulder) and 5.2 eV, which are not observed in the VUV absorption spectra. These energy losses have been ascribed to triplet states or optically forbidden singlet states.[39] Earlier CASPT2 calculations[40] located six optically forbidden singlet states in the range 4−5.5 eV, and the relation of these states with the present GVVPT2 calculations is shown in Table 6.

CASPT2 calculations[40] predict a 2^1B_{2g} state located at 5.48 eV. The GVVPT2 calculated value for this state is 5.78 eV, and extended STEOM-CC calculations place this state at 6.16 eV. Experimentally, the 2^1A_u state is located at 5.0 eV and CASPT2 calculates this state at 5.28 eV. Present GVVPT2 calculations locate the 2^1A_u state at 5.32 eV. Extended STEOM-CC calculates this state at 5.23 eV. For six low-lying states, the GVVPT2 and the CASPT2 excitation energy values differ by less than 0.05 eV. For states with excitation energy values above 5.3 eV, the GVVPT2 values are higher and are closer to the extended STEOM-CC calculated value.

4. Summary and Conclusions

Since the ability to predict excitation energies to within 0.5 eV of experimental results, using reasonable basis sets, makes a theory useful in assisting the assignment of experimental lines of molecules with complex spectra, we take this figure as a useful criterion on which to assess the GVVPT2 method. The results presented herein show that this goal has been reached in all cases in which an unambiguous comparison with experimental data can be made.

In the case of benzene, the valence excitation energies agree well with the experimental values, with a root-mean-square (rms) error of 0.22 eV. The results are in agreement with the latest CASPT2 values with the proposed shift of 0.25 au, although there are no *ad hoc* shifts used in the present method. For pyridine, maximum errors of 0.59 eV and 0.39 eV are seen for the $^1A_1$ ($n \rightarrow \pi^*$) and $^1B_1$ ($\pi \rightarrow \pi^*$) states, respectively. For pyridine, five states are calculated with an rms error of 0.32 eV. This lower accuracy is hardly surprising, since the earlier CASPT2 study,[15] which achieved good comparison with experiment, needed to use a significantly larger active space to describe these high-lying states. In the case of pyrazine, the singlet excitation energies for the $n \rightarrow \pi^*$ transitions are in better agreement with experimental values than the earlier CASPT2 values; the one $\pi \rightarrow \pi^*$ excitation energy considered agrees with the experimental values to within 0.11 eV. Our calculations also corroborate the CASPT2 prediction that the experimentally not observed ^1A_u state lies in between the $^1B_{3u}$ and $^1B_{2g}$ states.[15] For all triplet excitation energies considered (both $n \rightarrow \pi^*$ and $\pi \rightarrow \pi^*$), the rms error with the GVVPT2 approach is 0.23 eV. The $\pi \rightarrow \pi^*$ triplet excitation energies are obtained with an rms error of 0.29 eV, with the $n \rightarrow \pi^*$ being particularly accurate. Accuracies can also be assessed by considering maximum errors: the maximum error for the six singlet states is 0.11 eV and 0.34 eV for the five triplet states. For comparison, the maximum error for the triplets using SAC-CI SD-R is 0.8 eV and 0.66 eV using CASPT2. In the case of s-triazine, the excitation energy of $^1A_2''$, with the GVVPT2 approach, is underestimated by 0.4 eV; CASPT2 underestimates the excitation energy by 0.6 eV. We have maximum deviation of 0.47 eV from experimental results for the $^1E''$ state, although agree reasonably well with the EOM-CCSD(T) result which deviates by 0.59 eV; consequently, we support the observation made in the earlier CASPT2 study that the experimental data may be uncertain in this case. In the case of s-tetrazine, a maximum deviation of 0.51 eV is seen for the first ^1A_u state; a similar error of 0.54 eV is reported by the earlier CASPT2 study. GVVPT2 results are closer to the extended STEOM-CC results than the corresponding CASPT2 values. The GVVPT2 method predicts the excitation energies with an rms error of 0.35 eV for the valence $n \rightarrow \pi^*$ and $n,n \rightarrow \pi^*,\pi^*$ excited states.

In agreement with earlier applications of the GVVPT2 method, it is seen that the method is capable of providing useful results on problematic species. Using the same, moderate-sized active space for the $n \rightarrow \pi^*$ and $\pi \rightarrow \pi^*$ states, and without using potentially ambiguous shifts, the GVVPT2 approach predicts the excitation energies of the azabenzene series (i.e., benzene, pyridine, pyrazine, symmetric triazine and symmetric tetrazine) with an accuracy of 0.28 eV for all states considered. This study extends significantly demonstration of the applicability of the method.

Acknowledgment. The authors gratefully acknowledge the Department of Energy (Grant No. DE-FG02-04ER46120) for financial support of the research presented here.

References and Notes

(1) Khait, Y. G.; Song, J.; Hoffmann, M. R. *J. Chem. Phys.* **2002**, *117*, 4133.
(2) Song, J.; Khait, Y. G.; Hoffmann, M. R. *J. Phys. Chem. A* **2001**, *105*, 779.
(3) Pandey, R. R.; Khait, Y. G.; Hoffmann, M. R. *THEOCHEM* **2001**, *542*, 177.
(4) Dudley, T. J.; Hoffmann, M. R. *Mol. Phys.* **2003**, *101*, 1303.
(5) Song, J.; Khait, Y. G.; Wang, H.; Hoffmann, M. R. *J. Chem. Phys.* **2003**, *118*, 10065.
(6) Wang, H.; Khait, Y. G.; Hoffmann, M. R. *Mol. Phys.* **2005**, *103*, 257.
(7) Azenkeng, A.; Khait, Y. G.; Hoffmann, M. R. *Mol. Phys.* (in press).
(8) Jiang, W.; Khait, Y. G.; Hoffmann, M. R. *THEOCHEM* **2006**, *771*, 73.
(9) Innes, K. K.; Ross, I. G.; Moomaw, W. R. *J. Mol. Spectrosc.* **1988**, *132*, 492.
(10) Walker, I. C.; Palmer, M. H.; Hopkirk, A. *Chem. Phys.* **1989**, *133*, 113.
(11) Walker, I. C.; Palmer, M. H.; Hopkirk, A. *Chem. Phys.* **1990**, *141*, 365.
(12) Walker, I. C.; Palmer, M. H. *Chem. Phys.* **1991**, *153*, 169.
(13) Bolovinos, A.; Tsekeris, P.; Philis, J.; Pantos, E.; Andritsopoulos, G. *J. Mol. Spectrosc.* **1984**, *103*, 240.
(14) Andersson, K.; Malmqvist, P.-Å.; Roos, B. O.; Sadlej, A. J.; Wolinski, K. *J. Phys. Chem.* **1990**, *94*, 5483.
(15) Fülscher, M. P.; Andersson, K.; Roos, B. O. *J. Phys. Chem.* **1992**, *96*, 9204.
(16) Fischer, G. *Can. J. Chem.* **1993**, *71*, 1537.
(17) Kirtman, B. *J. Chem. Phys.* **1981**, *75*, 798.
(18) Khait, Y. G.; Hoffmann, M. R. *J. Chem. Phys.* **1998**, *108*, 8317.
(19) Malrieu, J. P.; Heully, J. L.; Zaitsevskii, A. *Theor. Chim. Acta* **1995**, *90*, 167.
(20) Khait, Y. G.; Song, J.; Hoffmann, M. R. *Int. J. Quantum Chem.* **2004**, *99*, 210.
(21) Khait, Y. G.; Jiang, W.; Hoffmann, M. R. Third order Generalized Van Vleck Perturbation Theory for Electron Correlation (to be submitted).
(22) *NIST Computational Chemistry Comparison and Benchmark Database*; Johnson, R. D., III, Ed.; NIST Standard Reference Database Number 101, Release 12; National Institute of Standards and Technology: 2005.
(23) Weber, P.; Reimers, J. R. *J. Phys. Chem. A* **1999**, *103*, 9821.
(24) Schütz, M.; Hutter, J.; Luth, H. P. *J. Chem. Phys.* **1995**, *103*, 7048.
(25) Dunning, T. H., Jr. *J. Chem. Phys.* **1989**, *90*, 1007.
(26) Widmark, P.-O.; Malmqvist, P.-Å.; Roos, B. O. *Theor. Chim. Acta* **1990**, *77*, 291.
(27) Pierloot, K.; Dumez, B.; Widmark, P.-O.; Roos, B. O. *Theor. Chim. Acta* **1995**, *90*, 87.
(28) Ghigo, G.; Roos, B. O.; Mamqvist, P.-A. *Chem. Phys. Lett.* **2004**, *396*, 142.
(29) Bernhardsson, A. Theoretical Studies of Response Properties of Organic Molecules; Thesis, University of Lund, 1999.
(30) Hiraya, A.; Shobatake, K. *J. Chem. Phys.* **1991**, *94*, 7700.
(31) Doering, J. P. *J. Chem. Phys.* **1977**, *67*, 6065.
(32) Goodman, L. *J. Mol. Spectrosc.* **1961**, *6*, 109.
(33) Nooijen, M; Bartlett, R. J. *J. Chem. Phys.* **1997**, *106*, 6441.
(34) Del Bene, J. E.; Watts, J. D.; Bartlett, R. J. *J. Chem. Phys.* **1997**, *106*, 3093.
(35) Li, Y.; Wan, J.; Xu, X. *J. Comput. Chem.* **2007**, *28*, 1658.
(36) Mason, S. F. *J. Chem. Soc.* **1959**, 1240.
(37) Mason, S. F. *J. Chem. Soc.* **1959**, 1263.
(38) Chawdhury, M.; Goodman, L. *J. Chem. Phys.* **1963**, *38*, 2979.
(39) Palmer, M. H.; McNab, H.; Reed, D.; Pollacchi, A.; Walker, I. C.; Guest, M. F.; Siggel, M. R. F. *Chem. Phys.* **1997**, *214*, 191.
(40) Rubio, M.; Roos, B. O. *Mol. Phys.* **1999**, *96*, 603.
(41) Nooijen, M. *J. Phys. Chem. A* **2000**, 104, 4553.
(42) Innes, K. K. *J. Mol. Spectrosc.* **1988**, *129*, 140.